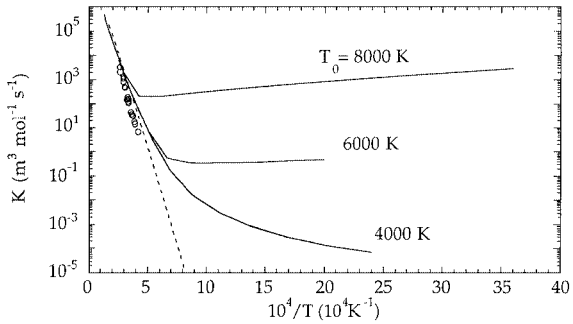

Fig. 4a NO global production rate for the reaction $N_2 + O \leftrightarrow NO + N$ and for different reservoir temperatures T_0. The symbols are experimental results,[10] and - - - - is their Arrhenius fit.

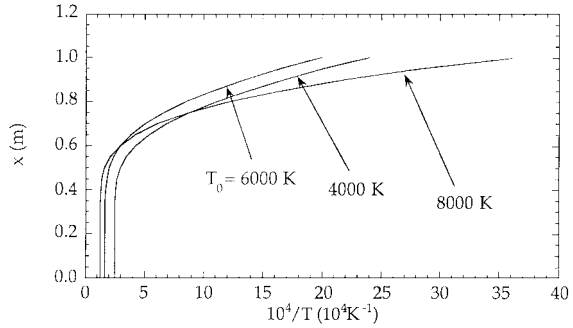

Fig. 4b Nozzle position as a function of the inverse of temperature along the nozzle axis.

Results obtained for nonparabolic nozzles (the so-called F4 nozzle operating at ONERA) closely follow those reported in Figs. 1–4, thus eliminating the uncertainties caused by the use of one-dimensional inviscid flow for parabolic nozzles.[9]

Conclusions

The results presented in this work have shown the role of nonequilibrium vibrational kinetics in the nozzle flow. In particular, the proposed model shows a strong non-Arrhenius character of the formation rate of NO through the reaction of vibrationally excited molecules and oxygen atoms. This behavior is mainly caused by the recombination of N atoms that form strong nonequilibrium vibrational distributions.

The present results, even though qualitative, represent a new attempt to describe nonequilibrium effects in nozzle expansion flows. Future work in this direction should be directed toward a better characterization of input data as well as to dedicated experiments able to monitor the concentration profiles of the different species as well as the vibrational distributions of diatomic molecules along the nozzle axis. Inclusion of these kinetics in two-dimensional nozzle flows should also improve the present treatment.

Acknowledgment

This Note has been partially supported by Agenzia Spaziale Italiana.

References

[1]Park, C., *Non-Equilibrium Hypersonic Aerothermodynamics*, Wiley, New York, 1990, pp. 326, 327.

[2]Armenise, I., Capitelli, M., Colonna, G., and Gorse, C., "Nonequilibrium Vibrational Kinetics in the Boundary Layer of Re-entering Bodies," *Journal of Thermophysics and Heat Transfer*, Vol. 10, No. 3, 1996, pp. 397–405.

[3]Colonna, G., and Capitelli, M., "Electron and Vibrational Kinetics in the Boundary Layer of Hypersonic Flow," *Journal of Thermophysics and Heat Transfer*, Vol. 10, No. 3, 1996, pp. 406–412.

[4]Capitelli, M., Armenise, I., and Gorse, C., "State-to-State Approach in the Kinetics of Air Components Under Re-Entry Conditions," *Journal of Thermophysics and Heat Transfer*, Vol. 11, No. 4, 1997, pp. 570–578.

[5]Bose, D., and Candler, G. V., "Thermal Rate Constants of the $N_2 + O \rightarrow NO + N$ Reaction Using *Ab Initio* 3A," *Journal of Chemical Physics*, Vol. 104, No. 8, 1996, pp. 2825–2833.

[6]Vincenti, W. G., and Kruger, C. H., Jr., *Introduction to Physical Gas Dynamics*, Wiley, New York, 1965, pp. 245–316.

[7]Giordano, D., Bellucci, V., Colonna, G., Capitelli, M., Armenise, I., and Bruno, C., "Vibrationally Relaxing Flow of N_2 Past an Infinite Cylinder," AIAA Paper 95-2072, June 1995; also *Journal of Thermophysics and Heat Transfer*, Vol. 11, No. 1, 1997, pp. 27–35.

[8]Colonna, G., "Step Adaptive Method for Vibrational Kinetics and Other Initial Value Problems," *Supplemento ai Rendiconti del Circolo Matematico di Palermo, Serie II*, No. 57, 1998, pp. 159–163.

[9]Colonna, G., Tuttafesta, M., Capitelli, M., and Giordano, D., "NO Formation in One-Dimensional Nozzle Air Flow with State-to-State Nonequilibrium Vibrational Kinetics," AIAA Paper 98-2951, June 1998.

[10]Monat, J. P., Hanson, R. K., and Kruger, C. H., "Shock Tube Determination of the Rare Coefficient for the Reaction $N_2 + O \rightarrow NO + N$," *Proceedings of 17th Symposium (International) on Combustion*, Combustion Inst., Univ. of Leeds, Leeds, England, UK, 1978, pp. 543–552.

View Factors Between Finite Length Rings on an Interior Cylindrical Shell

C. P. Tso* and S. P. Mahulikar†
Nanyang Technological University,
Singapore 639798, Republic of Singapore

Nomenclature

A	= surface area, m^2
D	= diameter, m
d	= distance, m
F_{i-j}	= view factor of surface j as seen by surface i
L	= length, m
r	= radius, m

Subscripts

b	= bottom surface
n	= neighboring surfaces
s	= shell surface
si	= shell interior surface
sid	= shell interior surface of length d
sn	= one of the neighboring shell surfaces
sTT	= total of two neighboring shell surfaces
TT	= total of two neighboring elements
t	= tube surface
u	= upper surface
1	= element 1
2	= element 2 or surface 2; Fig. 2a

Introduction

THE present work is aimed at analyzing surface radiation heat exchange in annular microchannels bounded by two coaxial heat-generating cylinders, for electronics cooling application. The geometry of coaxial cylinders is common to applications such as aircraft engines, heat exchangers, infrared telescopes, reactors, rockets, and tubular furnaces. The view factor, defined, e.g., by Siegel and Howell,[1] is a key element in the computation of radiant interchange between diffusely emitting surfaces. It is also used in conjunction with diffusion and transport codes to calculate the neutral particles

Received 11 August 1998; revision received 18 November 1998; accepted for publication 10 December 1998.

*Associate Professor, School of Mechanical and Production Engineering, Nanyang Avenue.

†Research Engineer, School of Mechanical and Production Engineering, Nanyang Avenue.

streaming through large voids surrounded by material regions.[2] The analytical evaluation of the view factor becomes complicated with complex geometry, and its numerical evaluation is time consuming for an adequate accuracy. This is especially true in practical applications involving systems discretized into a large number of spatial meshes viewing each other, for which several view factors are to be computed. Although software packages such as FACET and VIEW (discussed by Emery et al.[3]) compute the view factors numerically for complicated configurations, it is always advantageous to have closed-form analytical solutions wherever possible, to reduce the computation time and tedium, and to obtain insights of geometrical parameter dependence.

For analyzing the radiant heat exchange, the coaxial cylinders are discretized into coaxial ring elements. Leuenberger and Person[4] presented analytical solutions of view factors involving disks; finite length cylinders; and a combination of disks, cylinders, and rectangles. Their compilation includes the analytical expression for the differential view factor between a ring on the tube exterior and the finite annular space on the end plug between the tube and the coaxial shell. Reid and Tennant[5] performed a single numerical integration after three analytical integrations of the defining quadruple line integral, for ring elements on coaxial cylinders. They have numerically obtained the view factors between finite cylindrical areas on the interior of a shell, for cases 1 and 2 (Fig. 1) of the configuration from one shell interior surface to another. Rea[6] has derived, using view-factor algebra, the view factor between the outside of an end-capped cylinder to an annular disk plugged at its bottom, and presented the results for dimensionless geometrical parameters. The view-factor algebra for estimating the view factors between the exterior surface of a cylinder of smaller radius to the interior surface of a coaxial cylinder of larger radius was outlined. Siegel and Howell[1] have compiled a catalog of analytical solutions of view factors of several geometries, which includes the view factors for coaxial cylinders of the same finite length (F_{2-2} in Fig. 2a). Howell[7] has provided a more exhaustive coverage of geometries, some in the form of analytical expressions and some as numerical approximations or graphical solutions. The compilation includes some numerical results of Reid and Tennant[5] for the view factors between tube exterior and shell interior surfaces, and from one shell interior surface to another (cases 1 and 2 in Fig. 1). Brockmann[8] has obtained the view factors between the surface elements of two coaxial cylinders by replacing a surface integration in the view factor definition by integration over the direction of radiation emitted from that surface. Simplified expressions for known view factors (including for F_{2-2} in Fig. 2a) were also derived. Recently, Tso and Mahulikar[9] have shown the view factors for the two configurations, between the finite tube exterior and shell interior surfaces (configurations C-93 and C-95 in Howell[7]), to be identical.

In conclusion, the view-factor algebra for obtaining the view factors between shell interior surfaces separated by a finite distance has not been outlined, nor has a closed-form analytical solution been reported, although the configuration is of paramount importance in many practical applications. Also, case 3 of the configuration (to be described) has not been identified in the literature; hence, the motivation for the present work.

Derivation of Analytical Formulas for View Factors

Figure 1 shows the three cases of the view factor from one shell interior surface to another. In case 1 (Fig. 1a) the two shell-interior surfaces are separated by a distance, in case 2 (Fig. 1b) there is a partial overlap of the two shell interior surfaces, and in case 3 (Fig. 1c) one shell interior surface is completely inside the other. Although some of these cases may be encountered more often in practical applications than others, the view factor being a fundamental concept, it is of interest to study all of the cases analytically, as studied numerically by Reid and Tennant[5] for cases 1 and 2.

The view factors for the three cases will be derived analytically by a sequence of view-factor algebra. First the view factor between the two neighboring shell interior surfaces ($F_{sn1-sn2}$ in Fig. 2b) is derived, and it is used as a building block to derive the view factors for the three cases.

As illustrated in Fig. 2b, the shell interior surface is split into two neighboring surfaces ($sn1$ and $sn2$). By the conservation of radiant energy emitted by surface sTT toward itself,

$$F_{sTT-sTT} = F_{sTT-sn1} + F_{sTT-sn2} \tag{1}$$

By the reciprocal rule, $F_{sTT-sn1} = (A_{sn1}/A_{sTT}) \cdot F_{sn1-sTT}$, and $F_{sTT-sn2} = (A_{sn2}/A_{sTT}) \cdot F_{sn2-sTT}$. Hence, Eq. (1) may also be written as

$$F_{sTT-sTT} = (A_{sn1}/A_{sTT}) \cdot F_{sn1-sTT} + (A_{sn2}/A_{sTT}) \cdot F_{sn2-sTT} \tag{1a}$$

By the conservation of radiant energy emitted by surfaces $sn1$ and $sn2$ toward surface sTT, $F_{sn1-sTT} = F_{sn1-(sn1+sn2)}$, and $F_{sn2-sTT} = F_{sn2-(sn1+sn2)}$. Hence, Eq. (1a) may be written as

$$F_{sTT-sTT} = (A_{sn1}/A_{sTT}) \cdot F_{sn1-(sn1+sn2)} + (A_{sn2}/A_{sTT}) \cdot F_{sn2-(sn1+sn2)} \tag{1b}$$

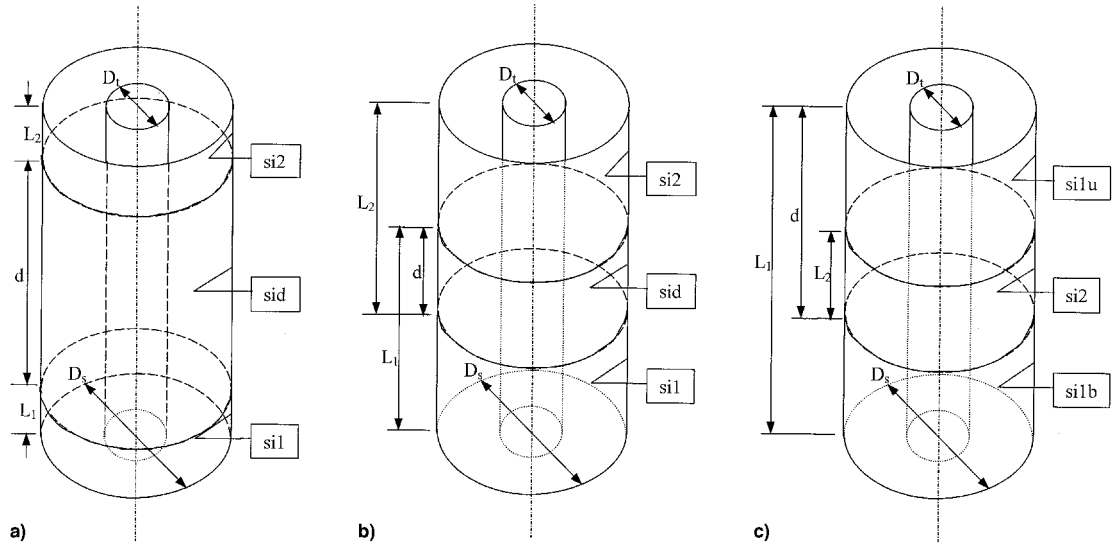

Fig. 1 Three cases of view factor from one shell interior surface to another: a) case 1: $d > 0$; b) case 2: $d < 0$, $(L_1 - |d|) > 0$, $(L_2 - |d|) > 0$; and c) case 3: $d < 0$, $(L_1 - |d|) > 0$, $(L_2 - |d|) < 0$.

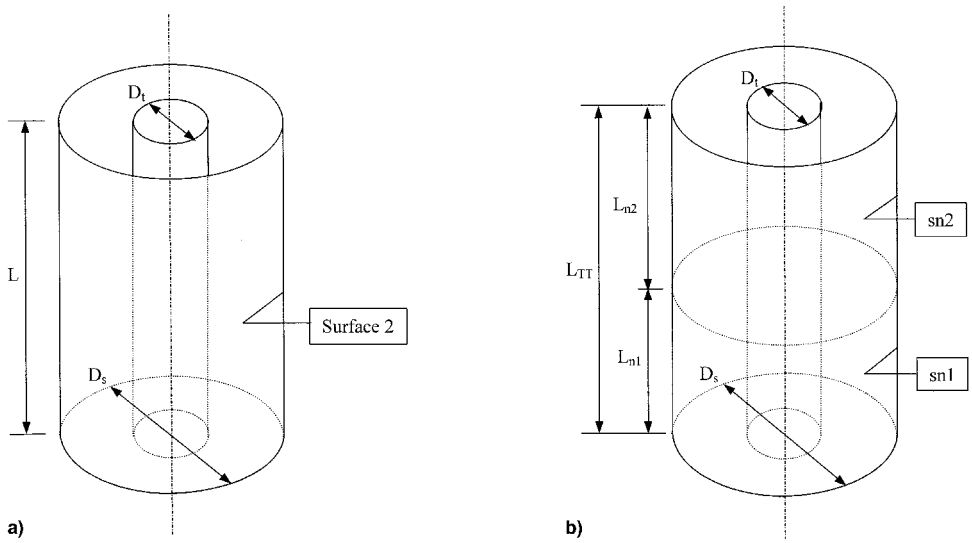

Fig. 2 Surfaces on coaxial cylinders: a) surfaces of coaxial cylinders of equal lengths and b) neighboring surfaces on shell interior of coaxial cylinders.

Because $F_{sn1-(sn1+sn2)} = F_{sn1-sn1} + F_{sn1-sn2}$, and $F_{sn2-(sn1+sn2)} = F_{sn2-sn1} + F_{sn2-sn2}$,

$$F_{sTT-sTT} = (A_{sn1}/A_{sTT}) \cdot (F_{sn1-sn1} + F_{sn1-sn2}) + (A_{sn2}/A_{sTT}) \cdot (F_{sn2-sn1} + F_{sn2-sn2}) \tag{1c}$$

However, $F_{sn2-sn1} = (A_{sn1}/A_{sn2}) \cdot F_{sn1-sn2}$, by the reciprocal rule, and the ratio of the areas is the same as the ratio of the lengths. Hence, Eq. (1c) is simplified to obtain

$$F_{sn1-sn2} = (L_{TT} \cdot F_{sTT-sTT} - L_{n1} \cdot F_{sn1-sn1} - L_{n2} \cdot F_{sn2-sn2})/(2 \cdot L_{n1}) \tag{2}$$

All of the view factors on the right-hand side (RHS) of Eq. (2) are known because they are for the same configuration (F_{2-2} in Fig. 2a). Hence, the view factor between two neighboring areas on the interior surface of a shell in the presence of an obstructing coaxial tube is known.

Case 1 ($d > 0$): Nonoverlapping Shell Segments

The view factor between areas on the interior surface of a shell separated by a distance d ($F_{si1-si2}$ in Fig. 1a) is written as (by the conservation of radiant energy)

$$F_{si1-si2} = F_{si1-(sid+si2)} - F_{si1-sid} \tag{3}$$

where the surfaces $(sid + si2)$ and sid are neighboring the surface $si1$, and hence, the view factors $F_{si1-(sid+si2)}$ and $F_{si1-sid}$ are of the same configuration as $F_{sn1-sn2}$ (Fig. 2b). Hence, the view factors on the RHS of Eq. (3) are known. The analytical formula for the view factor $F_{si1-si2}$ for case 1 is obtained by following the given view-factor algebra sequence, and the result is

$$F_{si1-si2} = \Big[(L_1 + L_2 + d) \cdot F_{(L_1+L_2+d)-(L_1+L_2+d)} - (L_1 + d) \cdot F_{(L_1+d)-(L_1+d)} - (L_2 + d) \cdot F_{(L_2+d)-(L_2+d)} + d \cdot F_{d-d}\Big]/(2L_1) \tag{4}$$

All of the view factors on the RHS are of configuration F_{2-2} (Fig. 2a), and the analytical expression for this view factor is provided by Siegel and Howell,[1] Leuenberger and Person,[4] Howell,[7] and Brockmann.[8] Because the form presented by Brockmann[8] appears to be the most compact, it is reproduced here as

$$F_{\xi} = \frac{1}{\pi X_{s\xi}}\left[\pi(X_{x\xi} - X_{t\xi}) + \cos^{-1}\frac{X_{t\xi}}{X_{s\xi}} - \sqrt{1 + 4X_{s\xi}^2} \cdot \tan^{-1}\frac{\sqrt{\left(1 + 4X_{s\xi}^2\right) \cdot \left(X_{s\xi}^2 - X_{t\xi}^2\right)}}{X_{t\xi}} + 2X_{t\xi} \cdot \tan^{-1}\left(2\sqrt{X_{s\xi}^2 - X_{t\xi}^2}\right)\right] \tag{4a}$$

where $X_{t\xi} = r_t/\xi$, and $X_{s\xi} = r_s/\xi$. With the length ξ taking different values $(L_1 + L_2 + d,\ L_1 + d,\ L_2 + d,\ d)$, a simple routine can be generated to calculate the required view factors.

Case 2 [$d < 0$, $(L_1 - |d|) > 0$, $(L_2 - |d|) > 0$]: Partially Overlapping Shell Segments

An analytical solution is similarly derived for case 2 (Fig. 1b). The spacing d shown in Fig. 1b is $|d|$, and the surface sid of length d is the partial overlap of the surfaces $si1$ and $si2$. By the conservation of radiant energy emitted by surface $si1$ toward $si2$,

$$F_{si1-si2} = F_{si1-sid} + F_{si1-(si2-d)} \tag{5}$$

Using the reciprocal rule for the view factor $F_{si1-sid}$, Eq. (5) can be written as

$$F_{si1-si2} = (d/L_1) \cdot F_{sid-si1} + F_{si1-(si2-d)} \tag{5a}$$

By the conservation of radiant energy emitted by surface sid toward $si1$, Eq. (5a) is

$$F_{si1-si2} = (d/L_1) \cdot \left[F_{sid-sid} + F_{sid-(si1-sid)}\right] + F_{si1-(si2-d)} \tag{6}$$

The view factor $F_{sid-sid}$ is of the same configuration as F_{2-2} (Fig. 2a), and the view factors $F_{sid-(si1-sid)}$ and $F_{si1-(si2-d)}$ are of the same configuration as $F_{sn1-sn2}$ (Fig. 2b). Because the view factors on the RHS of Eq. (6) are known analytically, the view factor $F_{si1-si2}$ for the configuration shown in Fig. 1b is obtained analytically. This view-factor algebra sequence is followed to obtain the analytical formula for the view factor $F_{si1-si2}$ (case 2):

$$F_{si1-si2} = \Big[(L_1 + L_2 - d) \cdot F_{(L_1+L_2-d)-(L_1+L_2-d)} - (L_1 - d) \cdot F_{(L_1-d)-(L_1-d)} - (L_2 - d) \cdot F_{(L_2-d)-(L_2-d)} + d \cdot F_{d-d}\Big]/(2L_1) \tag{7}$$

where the view factors F_ξ are as given by Eq. (4a) and the distance d in Eq. (7) is $|d|$.

Case 3 [$d < 0$, $(L_1 - |d|) > 0$, $(L_2 - |d|) < 0$]: Completely Overlapping Shell Segments

As shown in Fig. 1c, the surface $si2$ is completely inside the surface $si1$, thereby splitting the surface $si1$ into three parts: $si1b$, $si2$, and $si1u$. The spacing d shown in Fig. 1c is $|d|$. By the conservation of radiant energy emitted by surface $si2$ toward surface $si1$,

$$F_{si2-si1} = F_{si2-si1b} + F_{si2-si2} + F_{si2-si1u} \tag{8}$$

The three view factors on the RHS of Eq. (8) are known, because the view factor $F_{si2-si2}$ is of the same configuration as F_{2-2} (Fig. 2a), and the view factors $F_{si2-si1b}$ and $F_{si2-si1u}$ are of the same configuration as $F_{sn1-sn2}$ (Fig. 2b). These view factors are expanded as

$$\begin{aligned} F_{si1-si2} = \Big[&(L_1 + L_2 - d)\cdot F_{(L_1+L_2-d)-(L_1+L_2-d)} \\ &-(L-d)\cdot F_{(L_1-d)-(L_1-d)} - (d-L_2)\cdot F_{(d-L_2)-(d-L_2)} \\ &+ d\cdot F_{d-d}\Big]/(2L_1) \end{aligned} \tag{9}$$

where the view factors F_ξ are as given by Eq. (4a) and the distance d is $|d|$.

Equations (4) and (7) reduce to the same form as $d \to 0$. But Eq. (7) cannot be derived from Eq. (4) by simply changing the sign of d, because the geometries of cases 1 and 2 are different. Equation (9) reduces to $F_{L_1-L_1}$ (F_{2-2} in Fig. 2a) as $L_2 \to L_1$ and $d \to L_1$. Equations (4), (7), and (9) may be written succinctly as a single equation for all three cases as

$$\begin{aligned} F_{si1-si2} = \Big[&(L_1 + L_2 \pm |d|)\cdot F_{(L_1+L_2\pm|d|)-(L_1+L_2\pm|d|)} \\ &-|L_1 \pm |d||\cdot F_{|L_1\pm|d||-|L_1\pm|d||} - |L_2 \pm |d|| \\ &\times F_{|L_2\pm|d||-|L_2\pm|d||} + |d|\cdot F_{|d|-|d|}\Big]/(2L_1) \end{aligned} \tag{10}$$

where the signs preceding $|d|$ are positive for $d > 0$ (case 1), and they are negative for $d < 0$ (cases 2 and 3), except for the last term in the expression for which the sign is always positive.

Comparison of Results

The analytical solutions for cases 1 and 2 are used to generate results for different radius ratios (r_s/r_t), and they are compared in Fig. 3 with the numerical results for these two cases presented by Reid and Tennant.[5] For $(L_1 + d) > 2$, the results are for case 1 (Fig. 1a), and for $(L_1 + d) < 2$ the results are for case 2 (Fig. 1b). Figure 3 shows that the analytical results agree well with the reported numerical results. There is some difference between the two results for low values of (r_s/r_t) and $(L_1 + d) < 2$ (case 2), most likely because the effect of the obstruction is higher and the discretization for the reported numerical solution is not fine enough.

Figures 4a and 4b show the results for various r_s/r_t, keeping either r_t or r_s fixed, respectively. When r_s is increased at a fixed r_t, the effect of the obstruction reduces, but the percentage of radiation

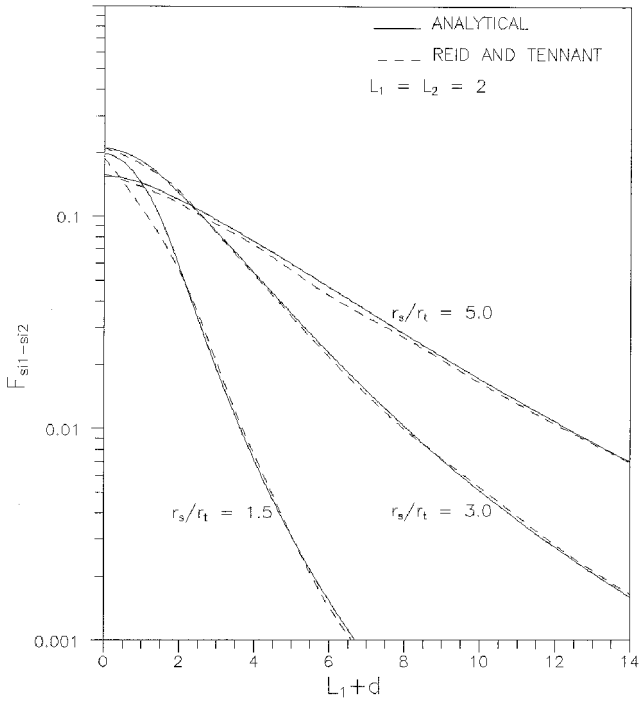

Fig. 3 View factors for shell interior surfaces: comparison with numerical results.

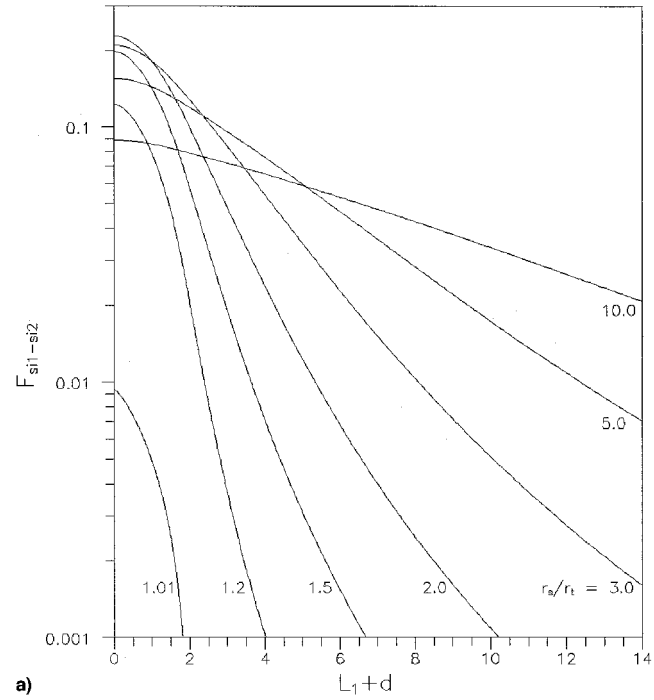

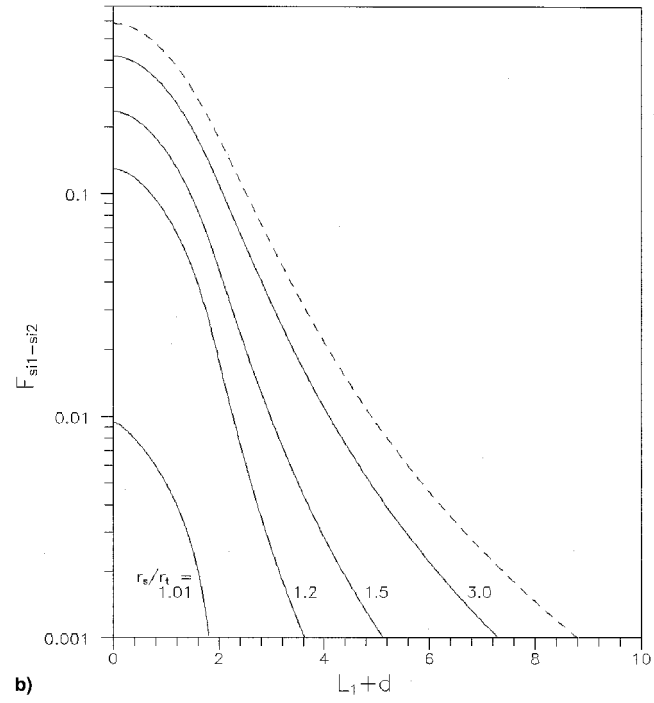

Fig. 4 View factors for shell interior surfaces, cases 1 and 2: a) $r_t = 1$, $L_1 = L_2 = 2$ and b) $r_s = 1$, $L_1 = L_2 = 2$.

incident on the cylindrical surface reduces, because more of the radiation is incident on the end-plugged annular disks. But if r_t is reduced at a fixed r_s, the percentages of radiation incident on the cylindrical surface and on the end-plugged annular disks increase, due to reduction of the obstruction. Hence, from Fig. 4a, $F_{si1-si2}$ is seen to go through an optimum with respect to r_s/r_t, for small values of d, whereas for larger values of d, it monotonically increases. This optimum is not observed in Fig. 4b. When r_t is fixed as in Fig. 4a and $(r_s/r_t) \to \infty$, $r_s \to \infty$, the shell reduces to a flat plate, and the surfaces $si1$ and $si2$ reduce to strips on the flat plate, for which $F_{si1-si2} = 0$ for any value of $(L_1 + d)$. However, when r_s is fixed as in Fig. 4b and $(r_s/r_t) \to \infty$, $r_t \to 0$ and $F_{si1-si2}$ reduces to the view factor between coaxial cylinders of equal radius without obstruction, derived analytically by Leuenberger and Person.[4] (This view factor is indicated by the dashed curve in Fig. 4b.) When r_s is fixed and $(r_s/r_t) \to 1$, the tube completely obstructs the radiation emitted by the shell, and $F_{si1-si2} = 0$. When both r_s and r_t are not fixed and both $(r_s, r_t) \to \infty$, $(r_s/r_t) \to 1$, and the two cylinders reduce to two flat plates, and again, $F_{si1-si2} = 0$. Also, when both $(r_s, r_t) \to 0$, $(r_s/r_t) \to 1$, and again, $F_{si1-si2} = 0$, because the inner tube completely obstructs the radiation. Hence, when the view factors are plotted for various r_s/r_t, the radius that is fixed must be specified.

The role of the tube in the view factor $F_{si1-si2}$ is limited to the radiation obstructed by it and not the reflected radiation. The reflected radiation is catered by the irradiation from the tube, and the amount incident on the shell surface is dictated by the view factor between tube exterior and shell interior surface elements, discussed by Tso and Mahulikar.[9]

Conclusion

The view factors for the three cases of shell interior surface segments are obtained analytically [Eqs. (4), (7), and (9)], and the analytical results agree well with the available reported numerical results. The results for the three cases can also be expressed by a single equation [Eq. (10)]. The analytical solutions are used to generate view factors for various radius ratios, which provide an insight into the complex nature of this view factor. The results generated for different radius ratios, keeping the tube and shell radius fixed separately, indicate differences, which implies that the radius that is fixed must also be specified.

Acknowledgment

The authors gratefully acknowledge the support provided by the National Science and Technology Board of Singapore, Project Number JTARC 5/96.

References

[1]Siegel, R., and Howell, J. R., *Thermal Radiation Heat Transfer*, McGraw–Hill, New York, 1992, pp. 980–1037.

[2]Brockmann, H., "Improved Treatment of Two-Dimensional Neutral Particle Transport Through Voids Within the Discrete Ordinates Method by Use of Generalized View Factors," *Deterministic Methods in Radiation Transport*, edited by A. F. Rice and R. W. Roussin, Oak Ridge National Lab., Oak Ridge, TN, 1992.

[3]Emery, A. F., Johansson, O., Lobo, M., and Abrous, A., "A Comparative Study of Methods for Computing the Diffuse Radiation Viewfactors for Complex Structures," *Journal of Heat Transfer*, Vol. 113, No. 2, 1991, pp. 413–422.

[4]Leuenberger, H., and Person, R. A., "Compilation of Radiation Shape Factors for Cylindrical Assemblies," American Society of Mechanical Engineers, Paper 56-A-144, 1956.

[5]Reid, R. L., and Tennant, J. S., "Annular Ring View Factors," *AIAA Journal*, Vol. 11, No. 10, 1973, pp. 1446–1448.

[6]Rea, S. N., "Rapid Method for Determining Concentric Cylinder Radiation View Factors," *AIAA Journal*, Vol. 13, No. 8, 1975, pp. 1122, 1123.

[7]Howell, J. R., *A Catalog of Radiation Configuration Factors*, McGraw–Hill, New York, 1982, pp. 89–220.

[8]Brockmann, H., "Analytic Angle Factors for the Radiant Interchange Among the Surface Elements of Two Concentric Cylinders," *International Journal of Heat and Mass Transfer*, Vol. 37, No. 7, 1994, pp. 1095–1100.

[9]Tso, C. P., and Mahulikar, S. P., "View Factor for Ring Elements on Coaxial Cylinders," *Journal of Thermophysics and Heat Transfer*, Vol. 13, No. 1, 1999, pp. 155–158.

Shock/Viscous Interaction Effects on Nonequilibrium-Dissociated Heating Along Arbitrarily Catalytic Surfaces

George R. Inger*
Iowa State University, Ames, Iowa 50011-3231

Nomenclature

C	$= \mu T_\infty/\mu_\infty T$, Chapman–Rubesin parameter
C_f	$= 2\upsilon_w/\rho_\infty U_\infty^2$, skin friction coefficient
C_p	= specific heat of the mixture
g	= net gas-phase reaction function (see Appendix)
H	= partial total enthalpy, $C_pT + u^2/2$
h_D	= dissociation energy per unit mass
$\hat{h}_D$	$= \beta^{1/4} h_D/P_R^{1/3}(H_{\text{ADIAB}} - H_w) C_{\text{REF}}^{1/8} \lambda^{3/4}(T_w/T_\infty)^{1/2}$
I_R	= reaction rate integral (see Appendix)
K_H	$= (\gamma+1)\lambda^{1/2} M_\infty^2 C_{\text{REF}}{}^{1/4} \varepsilon^2/4\beta^{1/2}$
K_w	= catalytic wall recombination velocity
L	= reference length (see Fig. 1)
M	= Mach number
P_R	= Prandtl number
p	= static pressure
q_D	= diffusive heat transfer; Eq. (24)
q_w	= wall heat transfer rate
R_u, R_m	= universal and molecular gas constants, respectively
Re_L	$= \rho_\infty U_\infty L/\mu_\infty$, Reynolds number $\equiv \varepsilon^{-8}$
S_c	= Schmidt number
s_e	= total streamline slope along the boundary-layer edge; Eq. (18)
T	= absolute static temperature
$\hat{T}$	$= \beta^{1/4}(T - T_w)/P_R^{1/3}(T_{\text{ADIAB}} - T_w)\varepsilon P_R^{1/3} C_{\text{REF}}^{1/8} \lambda^{3/4}(T_w/T_\infty)^{1/2}$
T_t	$= Ho_\infty/Cp$, freestream total temperature
U_∞	= freestream velocity at edge of incoming boundary layer
u, v	= velocity components in x, y directions, respectively
x, y	= streamwise and normal coordinates, respectively
α	= atom mass fraction
β	$= (M_\infty^2 - 1)^{1/2}$
Γ_c	= catalytic surface Damköhler number (see Appendix)
Γ_G, $\hat{\Gamma}_G$	= gas-phase Damköhler numbers (see Appendix)
$\tilde{\Gamma}_{i_w}$	$= C_{\text{REF}}^{1/8} \lambda^{1/4}(T_w/T_\infty)^{1/2} S_c^{1/3} \alpha_{e_0} \Gamma_{c0}/\beta^{1/4}(1 + \Gamma_{c0})$
γ	= specific heat ratio for frozen flow
δ^*	= displacement thickness variable
Θ	= flow deflection angle
λ	= 0.332 (Blasius solution constant)
λ_T	$= P_R^{1/3}(T_{\text{ADIAB}} - T_w)(1 + \Gamma_{c0})/S_c^{1/3} \alpha_{e_0}(1 - \Gamma_G I_R)\Gamma_{c0}$
μ	= coefficient of viscosity
ρ	= density
υ_w	= wall shear stress
ω	= viscosity temperature-dependence exponent ($\mu \sim T^\omega$)

Subscripts

ADIAB	= adiabatic wall conditions
B	= body surface
e	= local inviscid flow conditions at boundary-layer edge
i.s.	= incipient separation
REF	= based on reference temperature

Received 21 May 1998; presented as Paper 98-2814 at the AIAA 29th Fluid Dynamics Conference, Albuquerque, NM, 15–18 June 1998; revision received 26 February 1999; accepted for publication 2 March 1999.

*Professor, Department of Aerospace Engineering and Engineering Mechanics. Associate Fellow AIAA.